

Numerical Analysis of Impact Tests on Bending Failure of Reinforced Concrete Slabs Subjected to Inclined Soft Missile Impact

Christian Heckötter¹, Jürgen Sievers¹

¹Gesellschaft für Anlagen- und Reaktorsicherheit (GRS) gGmbH, Cologne, Germany

1 Abstract

Impact loading is a safety relevant loading case for reinforced concrete structures used to protect vital parts of nuclear facilities. Numerical methods used for the assessment are validated on the basis of impact tests. Even though normal impacts are the most common item of analysis, special issues are related to inclined impact. Effects of inclined impact include slipping and rotation of the missile, motion of the impact point and effects of tangential forces. Recently, an experimental program dealing with bending failure of reinforced concrete slabs subjected to inclined soft missile impact was carried out at Technical Research Centre of Finland (VTT) in the frame of phase IV of the international research project IMPACT. This paper reports on simulation results on these tests using LS-DYNA.

The numerical model is capable to reproduce the sliding of the missile above a critical angle of inclination and the utilized concrete models (***MAT_WINFRITH** and ***MAT_RHT**) are well suited to simulate the maximum deflections of the slab at several sensor locations. Regarding post impact vibration frequencies some differences occurred for ***MAT_RHT**. Progress has been achieved in simulation of strain measurements on reinforcement steel. Simulated spatial strain distribution tends to be more localized than the measured one.

2 Introduction

For the assessment of vital reinforced concrete structures of nuclear facilities subjected to impulsive loads, such as aircraft impact, it is common to distinguish hard and soft missile impact. If the deformability of the missile is large relative to the target, dynamics of missile and target may be treated uncoupled, and the missile is called a soft missile. According to Riera [1] inclined soft impact is of interest for three reasons:

1. It is not obvious, that normal impact is the most unfavourable regarding floor response spectra
2. The probability of normal impact is very low, which may be considered in new design criteria
3. Protective structures may prevent normal impact at critical points, which may be however subjected to inclined impact

Numerical tools used for the assessment of aircraft crash scenarios should be validated on the basis of impact tests. To the best of our knowledge, no experimental data on inclined soft missile impact on reinforced concrete targets was available. Due to this lack of data, a test program at the impact test facility [2] of the Technical Research Centre of Finland VTT was carried out in the framework of an international project called IMPACT (see e.g. [3], [4]). The tests of concern in this paper are hereinafter called IB-series tests and are dedicated to bending failure of reinforced concrete slabs. The present paper reports on simulation results of GRS on the IB-series using LS-DYNA software.

3 Experimental background

This section summarizes some details of the IB-series which are required for an understanding of the numerical modelling. A more comprehensive overview of IB-tests will be published elsewhere [5]. Basic test parameters of the four IB-series tests IB1-IB4 on inclined soft impact and two reference cases TF11 and TF12 dealing with normal impact are listed in Table 1. In this context the angle of inclination is measured between initial velocity of the cylindrical missile and surface normal of the target. Outer dimensions (2.1 x 2.1 x 0.15 m) and reinforcement of the target slabs were identical in all cases. Bending reinforcement is realised by A500HW bars with a diameter of 6 mm and a spacing of 50 mm each way and each face, while 410 closed shaped and evenly distributed stirrups serve as shear reinforcement. Further, design of the thin-walled stainless-steel missile (outer pipe diameter $\varnothing=254$ mm, total mass $M=50$ kg, total missile length $L=2150$ mm, sheet thickness about 2 mm) was identical in all cases. The

total mass is realised by a thicker pipe and a steel disk, which form the rear of the missile. In all cases the experimentally realised impact point was roughly the centre of the slab. In addition to these tests one force plate test FP11 with a relatively rigid target steel plate was performed to record the load time function for a soft impact with inclination of 20° and impact velocity of 114.6 m/s. Force plate test FP8 is dealing with normal impact at an impact velocity of 102.8 m/s.

Test no.	IB1	IB2	IB3	IB4	TF11	TF12
Impact velocity / ms ⁻¹	111.8	112.9	128.4	130.4	108.3	130.2
Inclination angle	20°	10°	20°	10°	0°	0°

Table 1: Basic test parameters of inclined bending (IB-series) soft missile impact tests.

Some details of the supporting systems are shown in Fig. 1. The slab is inserted in a frame which is horizontally supported at its corners by four back pipes against bedrock. Inclination of the target slab is realised by adapters. Cases with inclination require vertical supports. The boundary condition corresponds to a two-way simply supported slab with a span-width of 2 m, which is realised by eight rollers located between slab and target structure. With respect to the sliding of the missile, a wooden beam was used to protect the frame structure in IB1, while a steel plate was used in IB4 for this purpose. Among other things, instrumentation includes displacement sensors located on the rear face of the slab and strain gauges located on rear face bending reinforcement bars.

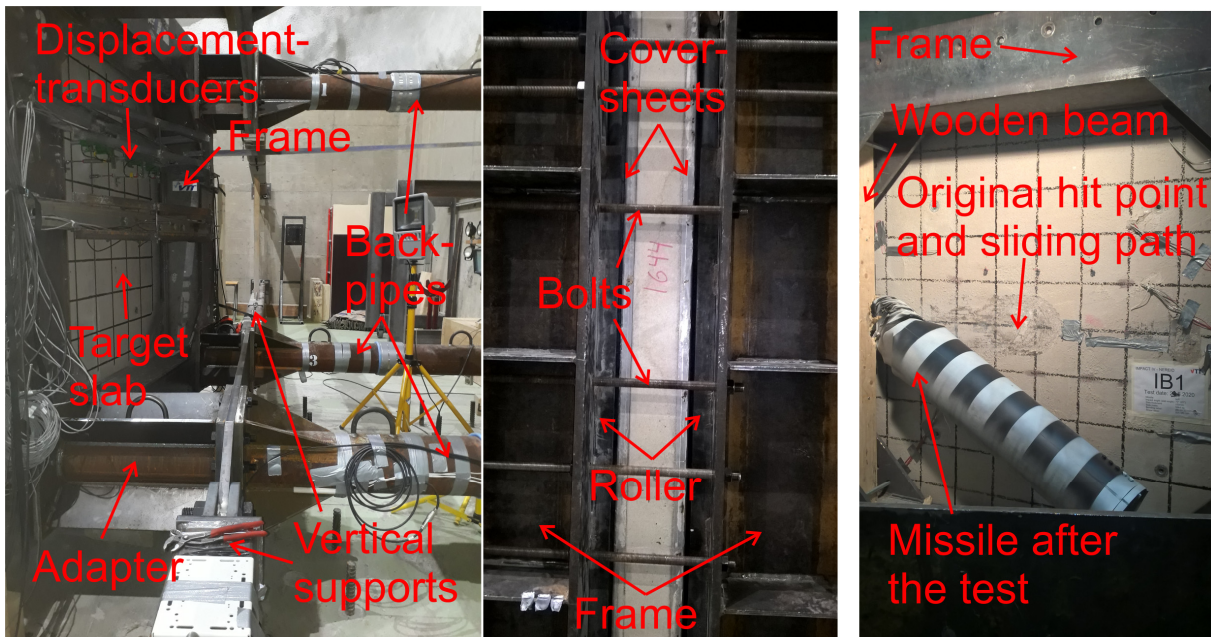


Fig.1: Details on experimental set-up on rear (left), side (middle) and front face (right) for IB1.

4 Numerical model

Fig. 2 shows some details of the numerical model developed by GRS for calculations with LS-DYNA. Concrete is discretized with an average element size of 12.5 mm using constant stress solid elements and standard viscous hourglass control. Reinforcement is represented by Hughes-Liu beam elements which are connected by means of joined nodes with concrete. Vertical and horizontal bending reinforcement bars are separated by a 7.5 mm thick layer of volume elements, while the concrete cover of 15 mm thickness is divided into two layers. Further, stirrups are not connected to bending reinforcement elements but separated to them by one layer of solid elements on each face. The intention of this refined meshing was to obtain a realistic representation of the spatial distribution of reinforcement strains. Prestressing of the bolts connecting front and rear face of the frame due to fastening torque is considered by means of *INITIAL_AXIAL_FORCE_BEAM Nodes at the location of the back pipe fixation are fixed using *BOUNDARY_SPC_SET. Fully integrated shell elements with a fine average element size of 4.5 mm were chosen to represent in detail the folding mechanism of the missile. For the

sake of reducing computational burden the missile is removed from the model using ***LOAD_REMOVE_PART_SET** after the load transfer is completed. The wooden beam of IB1 and the steel plate of IB2-IB4 are modelled in a simplified way by fixed solid elements filled with linear elastic material. Rollers are included in the model by solid elements to enable realistic rotations of the slab at the supports. Cover sheets are modelled with shells having shared nodes with concrete.

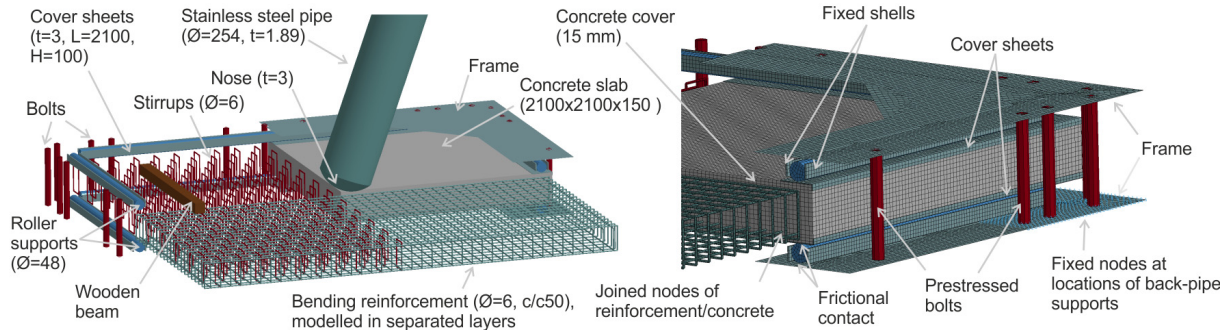


Fig. 2: Details of an LS-DYNA model used for inclined soft impact simulations (dimensions in mm).

Contacts ***CONTACT_AUTOMATIC_SURFACE_TO_SURFACE** are defined between missile/concrete, cover sheets/roller and frame/roller interfaces. Possible sliding of the missile is highly dependent on assumptions on friction coefficient μ_c as a function of relative velocities $|v_{rel}|$ of contact surfaces according to formula (1).

$$\mu_c = FD + (FS - FD)e^{-DC|v_{rel}|} \quad (1)$$

Parameters for the contact of missile to concrete were adjusted to $FD=0.15$, $FS=0.3$ and $DC=0.15$ s/m to match the observed missile behaviour of IB1 and IB2. It turned out, that this choice is capable to reproduce the behaviour of IB3 and IB4 as well (see section 5).

Material of missile and reinforcement steel is modelled using ***MAT_SIMPLIFIED_JOHNSON_COOK** [6] with input parameters listed in Table 2. The choice of strain rate constant C is based on experiments on reinforcement steel [7]. The same value is used for the missile material for pragmatic reasons. Remaining parameters were adjusted to test data on material characterisation supplied by VTT.

Parameter	RO	E	PR	A	B	N	C	EPS0
Rebars	7.85	210	0.3	590	2488	0.15	0.025	1.E-5
Stirrups	7.85	210	0.3	350	304	0.18	0.025	1.E-5
Missile	7.85	205	0.3	87	661	0.12	0.025	1.E-5
Unit	g/cm ³	GPa	-	MPa	MPa	-	-	s ⁻¹

Table 2: Input parameter sets of Johnson-Cook model (variables defined in [8]).

Concrete material properties were considered using ***MAT_WINFRITH** [9], which is examined in detail in [10]. Regarding tensile softening behaviour, both options for RATE were employed in the frame of a parametric study. Remaining parameters listed in Table 3 were adjusted to data on concrete characterisation supplied by VTT. The parameter ASIZE was chosen as the radius of the maximum aggregate size, not its diameter. This is mentioned due to ambiguity of [9] and [11] on meaning of ASIZE. Further, simulations using ***MAT_RHT** [11] model with input parameters adjusted according to [12] were performed as a parametric study on effects of concrete material modelling.

Parameter	RO	TM	PR	UCS	UTS	FE	ASIZE	RATE
Value	2.33	28.54	0.2	60	3.79	129 / 0.068	4	0 / 1
Unit	g/cm ³	GPa	-	MPa	MPa	Jm ⁻² / mm	mm	-

Table 3: Input parameter sets of Winfrith model (variables defined in [8]).

5 Results

Model views and high-speed camera images taken from bird's eye view at selected times are compared in Fig. 3 for tests IB3 and IB4. Apparently, pronounced sliding of the missile occurred in IB3. In the following the missile hits the frame structure, tilts and its heavy tail part is going to hit the slab. In IB4 the missile rebounds from the slab and only moderate displacement of the hit point occurred. Fig. 3 shows that the corresponding behaviour is satisfyingly reproduced by the numerical simulations. Similar results have been achieved for the tests IB1, FPI1 and IB2 with lower impact velocities.

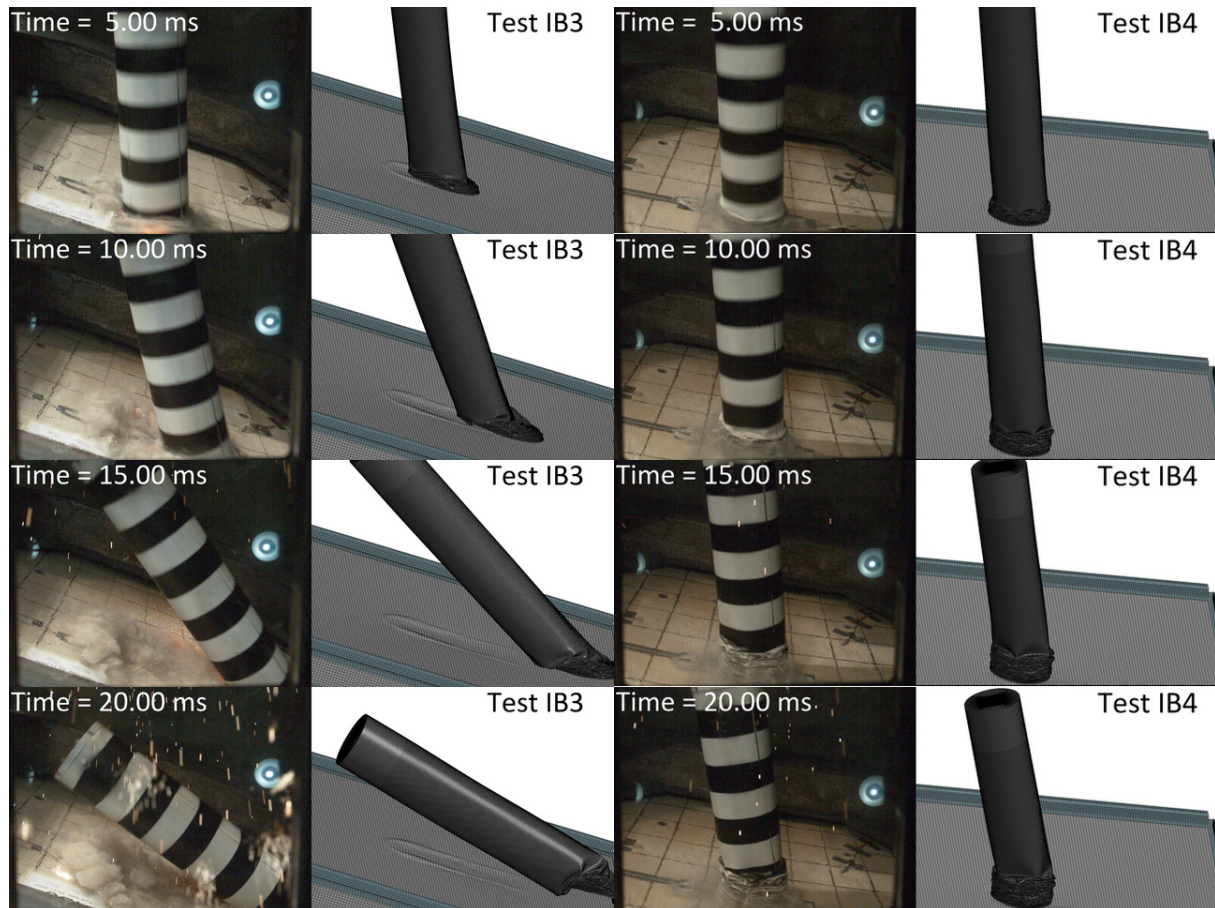


Fig.3: Comparison of missile behaviour in tests and simulations for test cases IB3 and IB4.

Corresponding kinematic test data provided by VTT are compared with simulation results in Fig. 4. Simulation results and test data regarding displacements of the impact point |OT| and current angles of inclination α agree reasonably well. Further, the simulations reproduce satisfyingly the crushing behaviour including number of folds, length of the folded segment as well as undeformed missile length.

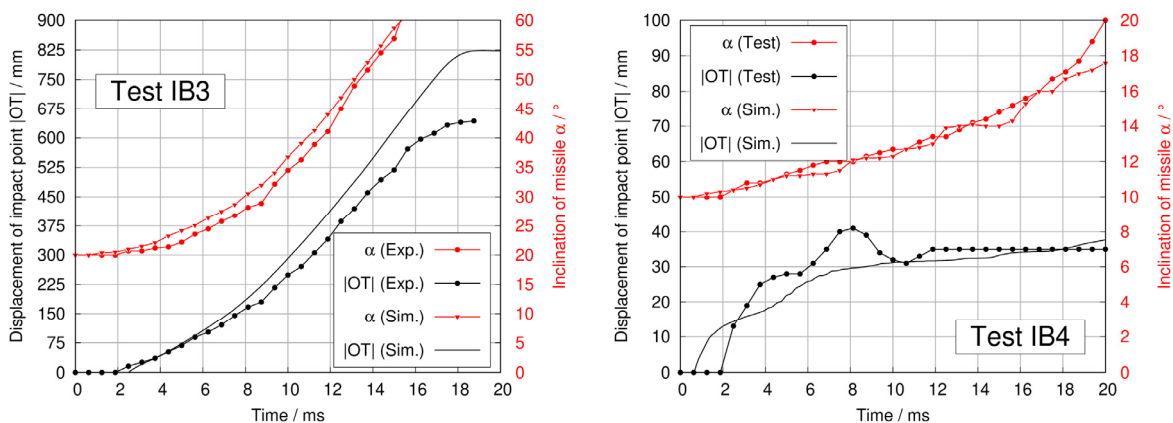


Fig.4: Comparison of measured and simulated kinematic data of the missiles in IB3 and IB4.

In tests with reinforced concrete target structures a direct measurement of impact forces is not possible. Therefore, Fig. 5 compares 1 kHz low pass filtered results of load cell signals in force plate tests FPI1 (inclination 20°) and FP8 (normal impact). These tests are comparable with IB1, IB2 and TF11 regarding impact velocity. Sliding of the missile and impact of the tail occurred in FPI1, while no sliding and rebound was observed in FP8. It should be noted that load cell signals include inertia effects of the force plate and are by trend somewhat larger than numerical contact forces. Further, load cell signals include tensile forces due to the oscillation of the force plate. It should also be noted that these tests deal with friction of a steel-to-steel interface. Even though the force plate was subjected to sandblasting prior to FPI1, some uncertainties regarding drawing conclusions for concrete slab tests remain. However, the comparison indicates a realistic choice of material properties as well as a viable choice of friction assumptions. After about 12 ms the missile slips of the force plate in IFP1. The impact of the rear occurs at about 24 ms. Both points in time are well captured by the simulation.

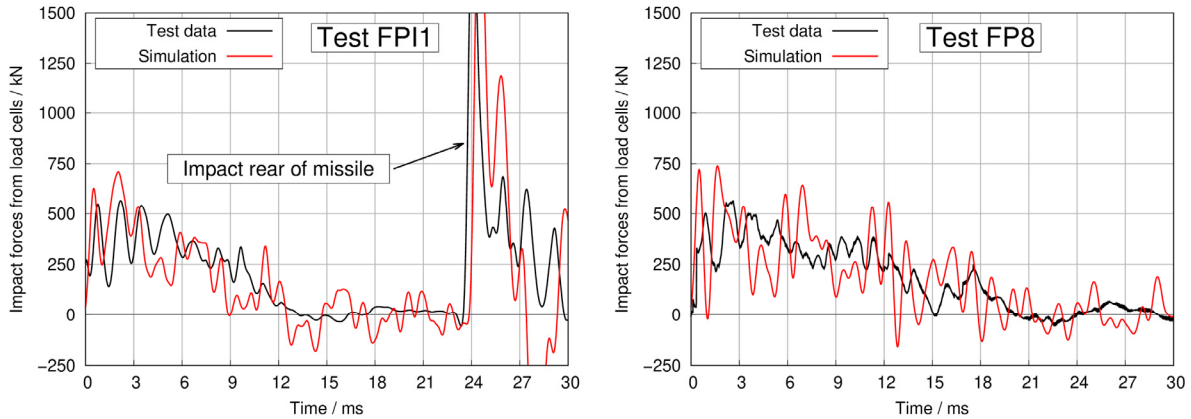


Fig.5: Comparison of numerical results on force plate test FPI1 and FP8 simulations with test data.

The effect of inclination on 1 kHz low pass filtered numerical contact forces normal to the slab is outlined in Fig. 6. Minor differences are visible between TF12 and IB4. Concerning impact duration, the resulting load-time-function agree very well with results obtained with the so-called Riera [13] method. Regarding peak forces, the Riera method yields an average impact force. This is illustrated by the comparison of momentum transfer. Due to some elastic energy and rebound of the missile the momentum transfer is somewhat larger in LS-DYNA simulations. The Riera method is based on a perfectly plastic shock and therefore results in a momentum transfer equal to the initial momentum. Due to the sliding of the missile in IB3, noticeable differences occur regarding load-time-function. A significant amount of momentum is not transferred and remains in the missile. The impact of the missile's rear after 24 ms is also apparent.

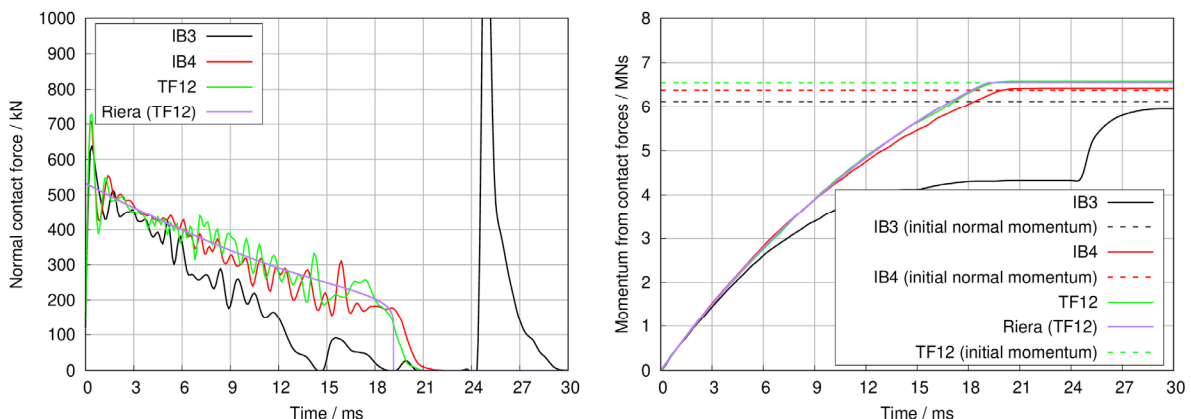


Fig.6: Comparison of numerical contact forces and momentum transfer for tests IB3, IB4 and TF12.

Damage of the back face of the slabs are compared in Fig. 7. For the RHT model contour plots of the damage parameter represent the damage status. In this context, red coloured elements correspond to fully damages material. The Winfrith model has the option of crack visualization, which is employed for the comparison. Cracks observed on the back face in the tests were highlighted with a marker. In all

cases diagonal crack patterns are observed. These cracks correspond to bending cracks along the yield line. In the view of Fig. 7 the sliding direction of the missile is to the right. Scabbing of concrete due to the impact of the rear of the missile is visible at the left-hand side of the centre of the slab in IB3. Crack patterns in IB4 are quite symmetric and only minor effects of inclination are visible in the simulation results. Crack patterns calculated by the Winfrith model are quite similar for the two options of RATE.

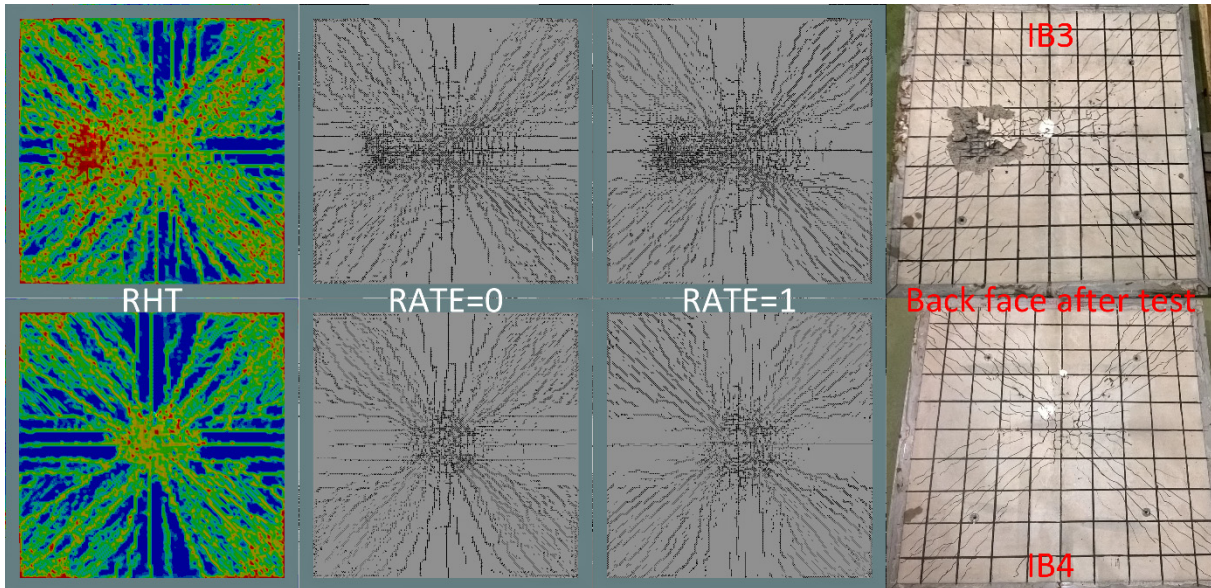


Fig.7: Comparison of back face slab damage after 100 ms and test results of tests IB3 and IB4.

Calculated and measured maximum central slab deflections during the first cycle of oscillation are compared in Fig. 8. In IB1 and TF12 the simulations overestimate the maximum deflection, while numerical and experimental results are consistent in the other cases. For TF12 the RHT model seems to overestimate central displacements and underestimate outer deflections (see Fig. 9). This might be due to some unrealistic prediction of punching deflection. It should be noted that test results of TF12 are questionable, since the beam that carried the displacement transducers was supposed to be too slender and started to oscillate during the test. Differences for IB1 may be attributed to some uncertainty regarding the hit point of the missile. An inclination of 10° seems to have very little influence on central deflection compared to cases with normal impact, which is consistent with the little effect on load-time-function (see Fig. 6). In cases IB1 and IB3 with sliding of the missile the effect compared to cases TF11 and TF12 is evident.

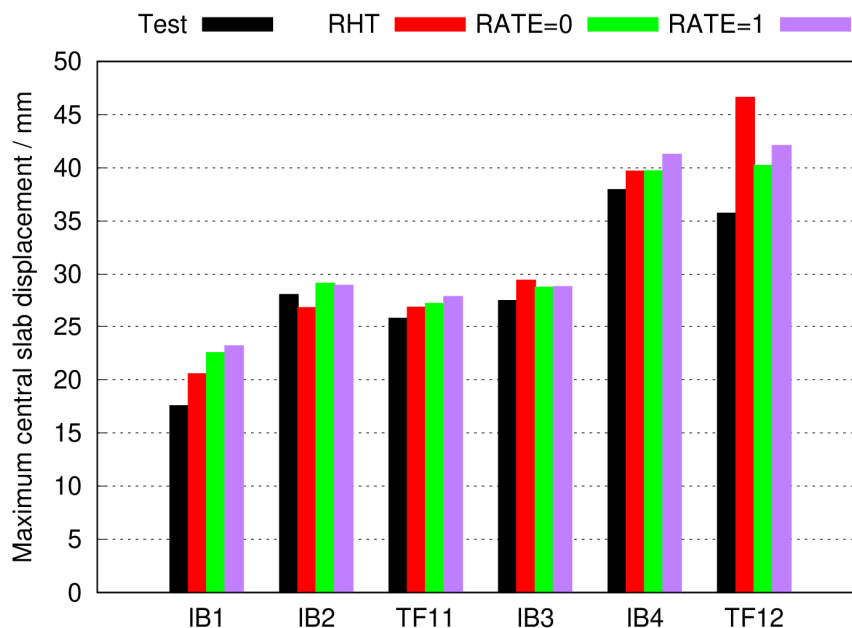


Fig.8: Comparison of maximum central slab displacements in the first cycle.

Time histories of back face slab displacements for two symmetrically located sensor locations are compared in Fig. 9 for tests IB3, IB4 and TF12. The sensor layout is shown as seen from the front, that is sliding occurs towards sensor D9. Both options for RATE of the Winfrith model are capable to reproduce maximum deflection as well as post impact vibration frequencies. From this result it is concluded that the stiffness of the cracked slab is very well predicted by the Winfrith model. Further improvement of the numerical result may require a more detailed modelling of the supporting frame. Regarding frequencies some deficits of the simulation with the RHT model are observed for IB4 and TF12. As mentioned above, test data for deflections in TF12 are questionable. Due to the inclination deflections at sensor location D9 are somewhat larger than those of D4. Especially for D4 the impact of the rear of the missile in IB3 is visible in test data and numerical results. This applies especially for sensor D4, which is closer to the impact location of the rear.

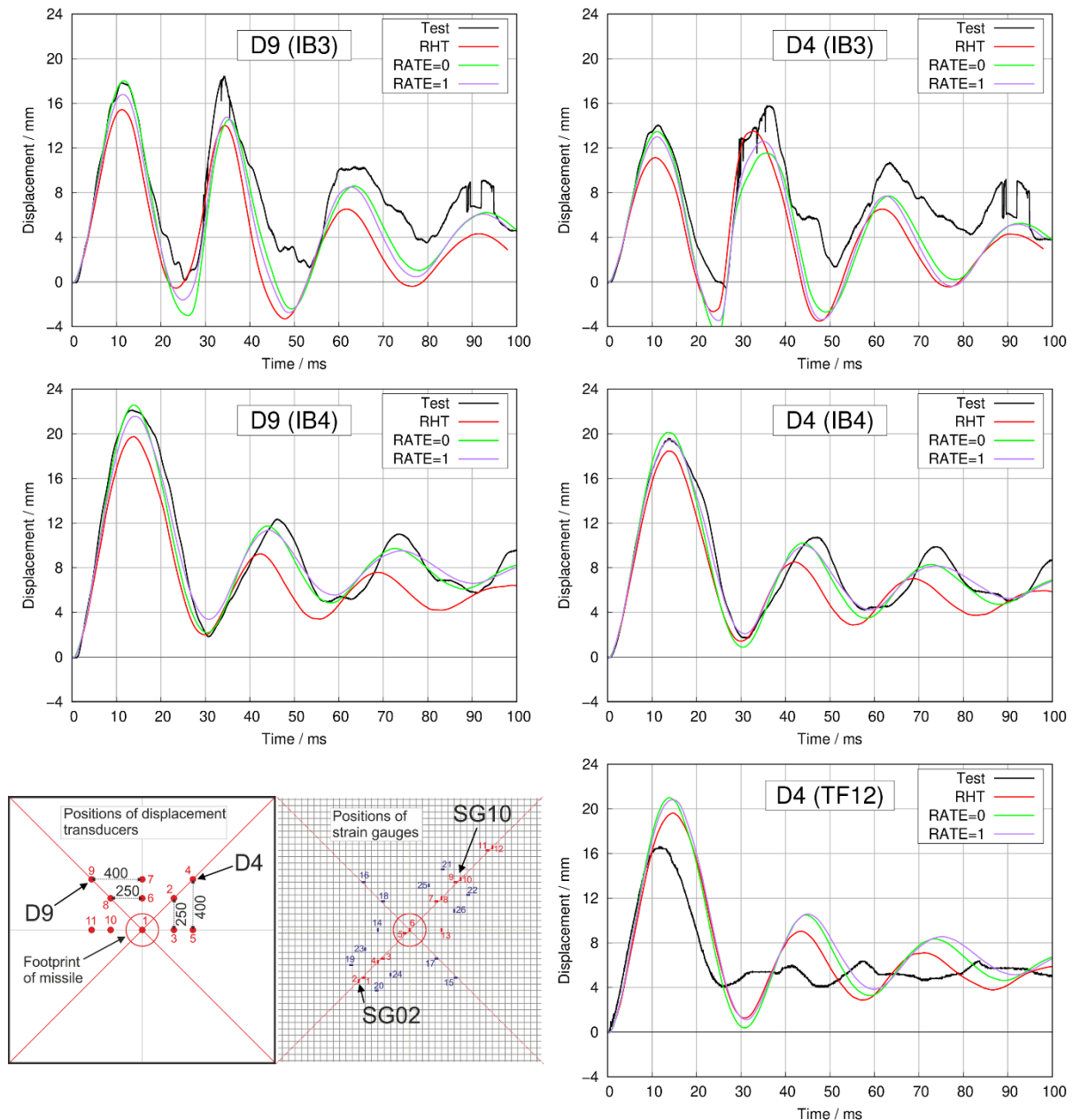


Fig.9: Calculated and measured back face slab displacements at selected sensor locations for IB3, IB4 and TF12.

Time histories of strains measured on back face reinforcement bars are displayed in Fig. 10 at strain gauge locations SG10 and SG02 specified in the layout shown in Fig. 9. Unfortunately, no test data were available for a strain gauge located close to sensor D9 for all the test cases. Therefore, the symmetrically located sensor SG02 is considered instead. In principle histories of strains are in phase

with histories of displacements. From this it can be concluded that bending failure is the dominant failure mode. It is apparent, that simulation results of strains are in less satisfying agreement with test data than results for displacements. In some cases, differences among the numerical results are observed, for instance at SG10 for IB4 or SG02 for TF12. It seems, that strains partly depend locally on positions of individual cracks of concrete or local buckles of reinforcement elements. The impact of the tail of the missile in IB3 is clearly visible in calculated and measured data of SG10.

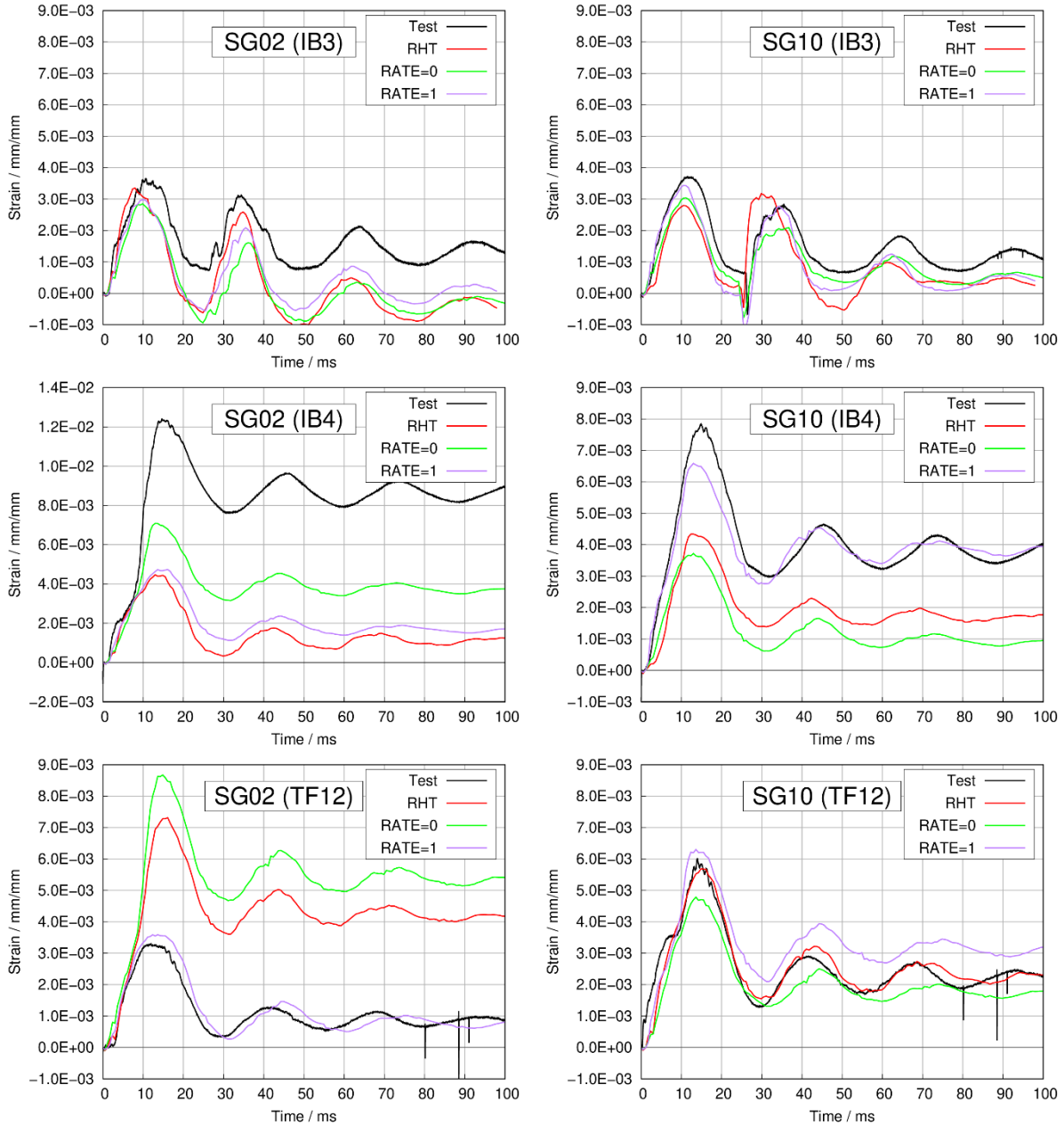


Fig. 10: Reinforcement strains at selected sensor locations for IB3, IB4 and TF12.

The conclusions on displacement and strain simulations are further illustrated in Fig. 11 with a comparison of spatial distributions after 15 ms. In these figures the current impact locations according to test data are indicated by missile perimeter lines. Fig. 11 is based on the layout of strain gauges shown in Fig. 9. All strain gauges were glued to the back face reinforcement inner surface. Exemplarily the results using RATE=0 of the Winfrith model were chosen for the comparison. Regarding test IB3 a certain overestimation of displacements in the direction of the sliding path of the missile is noticed, while displacements are slightly underestimated along the opposite direction. Notice, that in contrast to the test the largest calculated displacement of the first cycle after about 15 ms occurs at position of D10 ($x=-250$ mm, $y=0$ mm) and not in the centre. For test case IB4 the displacement distribution is very well

reproduced by the simulation, including sensor locations on the diagonal yield lines. On the other hand, reinforcement strains are reproduced satisfyingly only for a limited amount of strain gauges. Large strains are expected in the centre and on the diagonal yield lines. In fact, the largest strains over 6% with pronounced plastic deformation are observed in the centre. By trend the numerical results seem to be more localised than the test data. This applies especially for central strains of IB4. Some strain gauges failed during the test. In these cases, test data of zero are plotted in Fig. 11. It should be noted that similar findings were made for simulations with the RATE=1 option as well as the RHT concrete model. Also, the alternative method ***CONSTRAINED_BEAM_IN_SOLID** to couple reinforcement and concrete resulted in similar findings. This study illustrates that reinforcement strains seem to be more difficult to simulate than slab displacements for bending failure of reinforced concrete slabs. On the other hand, reinforcement strains are a key assessment criterion in aircraft crash analyses. Therefore, further studies should address the localisation of maximum strains in more details. In this context the influence of boundary conditions should be investigated. For instance, one-way slabs with slide bearing on two opposite edges and two unsupported edges should be analysed with respect to strain distribution. Furthermore, the effect of mesh-size should be studied in more details. Finally, the effect of damage should be analysed by consideration of tests with more pronounced target damage.

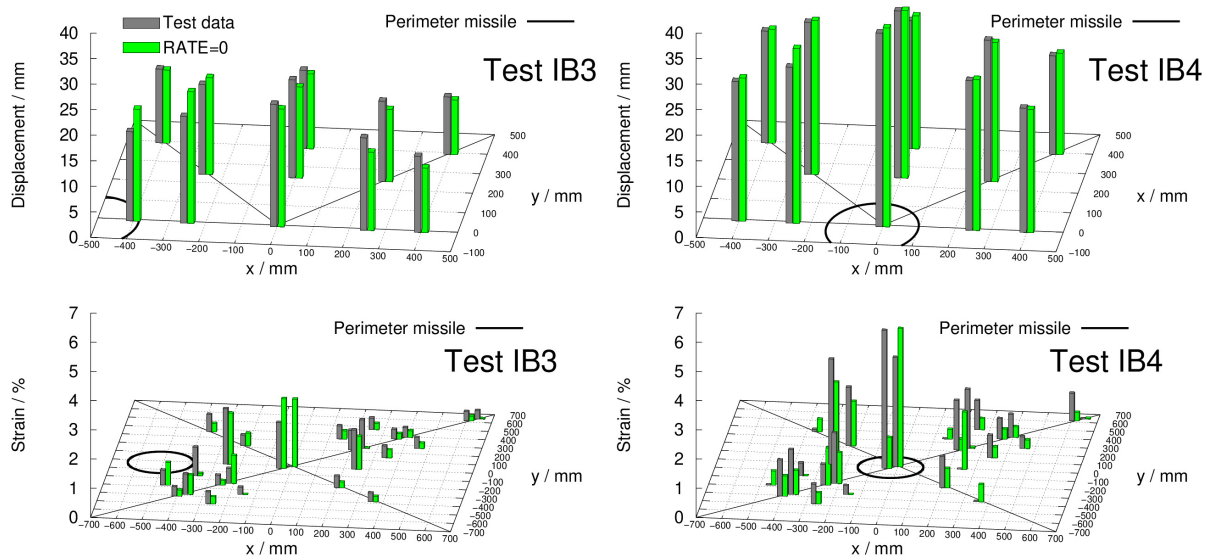


Fig.11: Comparison of measured and simulated spatial slab displacement and reinforcement strain distributions after 15 ms.

6 Summary

This paper presents numerical results of calculations with LS-DYNA on tests with reinforced concrete slabs subjected to inclined soft missile impact. The test series was carried out at Technical Research Centre of Finland VTT in the frame of the international project IMPACT. The predominant failure mode of the slabs is bending failure.

For an angle of inclination of 20° degree the missile slides and rotates, while only small impact point displacements occur for 10° of inclination. The numerical simulation is capable to reproduce the kinematic behaviour as well as the crushing mechanism of the missile. Related load-time-functions are supposed to be realistic.

Concrete crack patterns and maximum slab displacements are well predicted by ***MAT_WINFRITH** and ***MAT_RHT**. In this context ***MAT_WINFRITH** yields a slightly better representation of post impact vibration frequencies than ***MAT_RHT**.

In comparison with slab displacements, strains of back face reinforcement seem to be more difficult to reproduce. A satisfying agreement is only found for a limited number of strain gauge locations. This may be attributed to local effects of concrete cracks and buckling of rebars. Especially in areas with larger plastic strains the simulation results seem to be more localised than the test data.

7 Acknowledgement

The work was carried out in the frame of the German reactor safety research program funded by the German Federal Ministry for Economic Affairs and Energy (BMWi).

8 Literature

- [1] Riera, J. D.: "A critical reappraisal of nuclear power plant safety against accidental aircraft impact", Nuclear Engineering and Design 57, 1980, 193-206
- [2] Lastunen, A. et al.: "Impact Test Facility", 19th International Conference on Structural Mechanics in Reactor Technology (SMiRT-19), Paper #J08/2, Toronto, Canada, 2007
- [3] Tarallo, F., Rambach, J.-M.: "Some Lessons Learned from Tests of VTT IMPACT Program Phases I and II", 22nd International Conference on Structural Mechanics in Reactor Technology (SMiRT-22), San Francisco, USA, 2013
- [4] Tarallo, F. et al.: "Reinforced Concrete Slab under Soft Missile Impact at Medium Speed: Lessons Learned from VTT IMPACT Project", 25th International Conference on Structural Mechanics in Reactor Technology (SMiRT-25), Charlotte, USA, 2019
- [5] Technical Research Centre of Finland VTT.: "IMPACT IV – NEREID IB test series report", research report VTT-R-00359-21, Confidential, 2021. It is intended to present some aspects during the 26th International Conference on Structural Mechanics in Reactor Technology (SMiRT-26) in Potsdam/Berlin, Germany.
- [6] Johnson, R. J., Cook, W. H.: "Constitutive Model and Data for Metals Subjected to Large Strains, High Strain Rates and High Temperatures", 7th Int. Symposium on Ballistics, 1983
- [7] Amman, W.: "Zugversuche an Bewehrungs- und Spannstahl mit erhöhter Dehngeschwindigkeit", Bericht 7709-1, Institut für Baustatik- und Konstruktion ETH Zürich, 1982
- [8] LS-DYNA Keyword User's Manual Volume II, Material Models, LS-DYNA R11, 2018
- [9] Broadhouse, B.J., Attwood, G.J.: "Finite Element Analysis of the Impact Response of Reinforced Concrete Structures Using DYNA3D", 12th International Conference on Structural Mechanics in Reactor Technology (SMiRT-12), Paper JH13/3, Stuttgart, Germany, 1993
- [10] Schwer, L.: "The Winfrith Concrete Model: Beauty or Beast? Insights into the Winfrith Concrete Model", 8th European LS-DYNA Users Conference, Strasbourg, France, 2011
- [11] Borrval, T., Riedel, W.: "The RHT Concrete Model in LS-DYNA", 8th European LS-DYNA Users Conference, Strasbourg, France, 2011
- [12] Heckötter, C., Sievers, J.: "Comparison of the RHT concrete material model in LS-DYNA and ANSYS AUTODYN", 11th European LS-DYNA Conference, Salzburg, Austria, 2017
- [13] Riera, J. D.: "On the Stress Analysis of Structures Subjected to Aircraft Impact Forces", Nuclear Engineering and Design 8, 1968, 415-426